

CloudSat Project

A NASA Earth System Science Pathfinder Mission

Level 2 Fluxes and Heating Rates Product Process Description and Interface Control Document

Version: 5.1

Date: October 8, 2007

Questions concerning the document and proposed changes shall be addressed to:

Tristan L'Ecuyer tristan@atmos.colostate.edu



**Cooperative Institute for Research in the Atmosphere
Colorado State University
Fort Collins, CO 80523**

Approvals

_____ Date _____
Tristan L'Ecuyer
Data Product Algorithm Lead

_____ Date _____
Deborah Vane
Deputy Project Scientist

_____ Date _____
Graeme Stephens
Project Scientist

_____ Date _____
Donald Reinke
Data Processing Center Lead Engineer

_____ Date _____
TBD
"Receivers(s) of this data up the Level 2 chain"

Questions concerning the document and proposed changes shall be addressed to:

Tristan L'Ecuyer
tristan@atmos.colostate.edu
+1 970 491 8370

Contents

| | | |
|----------|--|-----------|
| 1 | Introduction | 4 |
| 2 | Algorithm Theoretical Basis | 4 |
| 2.1 | Overview | 4 |
| 2.2 | Radiative Transfer Model | 4 |
| 2.2.1 | Two-stream formulation | 4 |
| 2.2.2 | Method of solution | 5 |
| 2.2.3 | Implementation | 6 |
| 3 | Algorithm Inputs | 7 |
| 3.1 | CloudSat Level 2 Products | 7 |
| 3.2 | Ancillary Data Sets | 8 |
| 3.2.1 | Atmospheric State Variables | 8 |
| 3.2.2 | CloudSat Ancillary Albedo Dataset | 8 |
| 3.2.3 | Ancillary MODIS Data | 8 |
| 3.3 | Control and Calibration | 9 |
| 4 | Algorithm Summary | 9 |
| 4.1 | Pseudo-code | 9 |
| 4.2 | Algorithm Parameters | 10 |
| 4.3 | Algorithm Performance | 10 |
| 4.3.1 | Timing Requirements and Performance | 10 |
| 4.3.2 | Uncertainty Requirements and Performance | 10 |
| 5 | Data Product Output Format | 11 |
| 5.1 | Data Contents | 11 |
| 5.2 | Data Format Overview | 12 |
| 5.3 | Data Descriptions | 12 |
| 6 | Example | 17 |
| 7 | Operator Instructions | 18 |
| 8 | Changes Since Version 5.0 | 19 |
| 9 | Acronym List | 20 |

1 Introduction

This document provides an overview of the 2B-FLXHR flux and heating rate algorithm for CloudSat. The objective of the algorithm is to make use of liquid and ice water content estimates from the CloudSat Profiling Radar (CPR) to produce estimates of broadband fluxes and heating rates for each radar profile. For a particular radar profile, upwelling and downwelling longwave and shortwave flux profiles are calculated at discrete levels of the atmosphere. Corresponding heating rates are inferred from these fluxes. In order to perform these calculations, the algorithm makes use of a combination of atmospheric state variables obtained from ECMWF reanalysis data, profiles of cloud ice and liquid water content obtained from the CloudSat 2B-LWC and 2B-IWC products, and surface albedos obtained from seasonally-varying maps of surface reflectance properties. The remainder of this document describes the algorithm in greater detail. Section 2 provides an overview of the theoretical basis upon which the algorithm is built. Sections 3 and 4 describe inputs to the algorithm and detail its implementation. The output format for the product is summarized in Section 5 while instructions for the operator can be found in Section 6.

2 Algorithm Theoretical Basis

2.1 Overview

The core of the algorithm employs a broadband, two-stream, plane-parallel doubling-adding radiative transfer model. The general structure of the algorithm is similar to that described by Ritter and Geleyn [4]. The particular parameterizations and performance of the algorithm are described by Stephens et al. [1]. The model utilizes a delta-Eddington formulation in six shortwave bands and a constant-hemisphere formulation in twelve longwave bands. An appropriate set of atmospheric state variables and retrieved cloud ice/liquid water contents are used to calculate the vertical profile of band-resolved optical properties. These optical properties are then used to describe the reflectance (R), transmission (T) and radiative source (Σ) characteristics of each slab. By combining R , T , and Σ systematically for multiple slabs using the interaction principle, the broadband radiative fluxes at each slab face can be calculated. By calculating the amount of flux absorbed or emitted by each slab, the rate of radiative heating in each slab can be determined. Finally, the broadband fluxes and heating rates are aggregated to the spectral resolution of the 2B-FLXHR product and reported with the required vertical resolution.

2.2 Radiative Transfer Model

2.2.1 Two-stream formulation

The optical properties for a single homogeneous slab can be described in terms of its bulk, or “global”, bidirectional reflectance, R , global bidirectional transmission, T , and global radiative source properties, Σ . For such a slab with faces labelled “ a ” and “ b ”, once R , T , and Σ are determined the solution to the two-stream monochromatic radiative transfer equation can be written as:

$$F_a^+ = RF_a^- + TF_b^+ + \Sigma^+$$

$$F_b^- = RF_b^+ + TF_a^- + \Sigma^-$$

where superscript “+” indicates a quantity directed in the “ $b \rightarrow a$ ” direction and a superscript “-” indicates a quantity directed in the “ $a \rightarrow b$ ” direction. Given the fluxes F_a^- and F_b^+ at the layer boundaries, the two remaining fluxes can be determined. For an n -layer atmosphere, a tridiagonal system of $2n+2$ coupled equations can be written in similar form and solved recursively using the adding relations described by Stephens and Webster [2]. Stephens et al. [1] show that the computational expense for this sort of scheme increases linearly with the number of atmospheric layers, making it attractive for use on data which is highly vertically resolved, such as that that will be produced by CloudSat.

R , T , and Σ depend on the optical depth, τ , the single scattering albedo, ω_0 , (the ratio of the scattering coefficient to the extinction coefficient) and the asymmetry parameter g (the fraction of the incident energy that is scattered in the forward direction) of the matter in the layer. The particular form of R , T , and Σ depend on the nature of the radiative source and on which formulation is being used. In the solar wavelengths, the radiative source is due to scattering of the direct solar beam and the delta-Eddington method is employed. In the longwave spectrum, the radiative source is due to thermal emission of the atmosphere and the constant hemisphere method is used. Stephens et al. [1] studied a range of radiative transfer scenarios produced by a global climate model and evaluated the performance of two-stream delta-Eddington, two-stream constant hemisphere, and four-stream solution techniques. For the bulk of the solar radiative transfer scenarios, the

delta-Eddington method produced superior results compared to the other two. For longwave radiative transfer, the constant hemisphere method proved superior.

To obtain τ , ω_0 , and g for the layer as a whole, the optical properties of the components of the layer must be evaluated. In general, τ , ω_0 , and g for each material will vary spectrally but this spectral variation over some of the narrow spectral bands, employed in the 2B-FLXHR algorithm is negligible. Consequently, while some optical properties must be treated as spectrally variant, others, where possible, are approximated to be grey (invariant within the spectral band) in the interest of computational efficiency. In general, layer τ , ω_0 , and g can include any combination of the following processes: Rayleigh scattering, gaseous absorption, and both absorption and scattering by condensed water.

2.2.2 Method of solution

The 2B-FLXHR radiative transfer algorithm performs independent flux calculations over twelve longwave bands and six solar bands. These bands are summarized in Table 1. Ultimately these bands are combined into the two broadband flux estimates, one over the longwave and the other over the shortwave, that are ultimately reported by the algorithm.

Table 1: Bands used by 2B-FLXHR.

| Longwave (LW) | | Shortwave (SW) | |
|----------------------|-------------------|----------------------|-------------------|
| Band Limits, μm | corr. k Intervals | Band Limits, μm | Corr. k Intervals |
| 4.55 - 5.26 | 2 | 0.20 - 0.69 | 10 |
| 5.26 - 5.88 | 3 | 0.69 - 1.23 | 8 |
| 5.88 - 7.14 | 4 | 1.23 - 1.90 | 12 |
| 7.14 - 8.00 | 4 | 1.90 - 2.50 | 7 |
| 8.00 - 9.09 | 3 | 2.50 - 3.51 | 12 |
| 9.09 - 10.20 | 5 | 3.51 - 4.00 | 5 |
| 10.20 - 12.50 | 2 | | |
| 12.50 - 14.92 | 10 | | |
| 14.92 - 18.51 | 12 | | |
| 18.51 - 25.00 | 7 | | |
| 25.00 - 35.71 | 7 | | |
| 35.71 - ∞ | 8 | | |

The principal steps in the execution of the 2B-FLXHR algorithm are summarized in Figure 1. Calculations are done for each band sequentially. For each band, the algorithm proceeds by first computing and combining the optical properties for the gases in each atmospheric layer. Then a loop over spectral intervals is performed in which the spectrally varying cloud optical properties are computed, combined with the atmospheric optical properties, then used in a two-stream calculation to compute the fluxes in the spectral interval. As the loop continues, the spectral fluxes are summed to produce the band flux, then the band heating rates are computed. The set of shortwave and longwave fluxes and heating rates are then output at the maximum vertical resolution of the CPR and the 2B-CWC product, i.e. 240 m. This output forms the 2B-FLXHR product.

For the solar bands, molecular (Rayleigh) scattering and condensed water optical properties are treated as grey properties. Rayleigh optical thicknesses for all layers are calculated using a parameterization based on the central wavelength of the band, the layer pressure, and the pressure thickness of the layer. Additionally, refractive effects are considered in the visible band. The optics of condensed water particles are obtained from anomalous diffraction theory (ADT) using parameterizations derived from Stephens et al. [5] and Mitchell et al. [6]. Cloud particle distributions are described using a modified gamma size distribution with effective radii of 10 μm for liquid droplets and 30 μm for ice particles.

For longwave bands, the condensed water optics are considered grey along with water vapor continuum absorption and Planck emission. Condensed water optics are parameterized using ADT as mentioned above with the exception that, for longwave bands, precalculated values of asymmetry parameters for each band are used. Absorption by the water vapor continuum is treated using a parameterization developed from the water vapor continuum of CKD 2.1 by Clough et al. [7]. The general method of implementation for the correlated-k treatment of the gaseous absorption is described by Lacis and Oinas [8]. The details of this particular implementation are described in Fu and Liou [3].

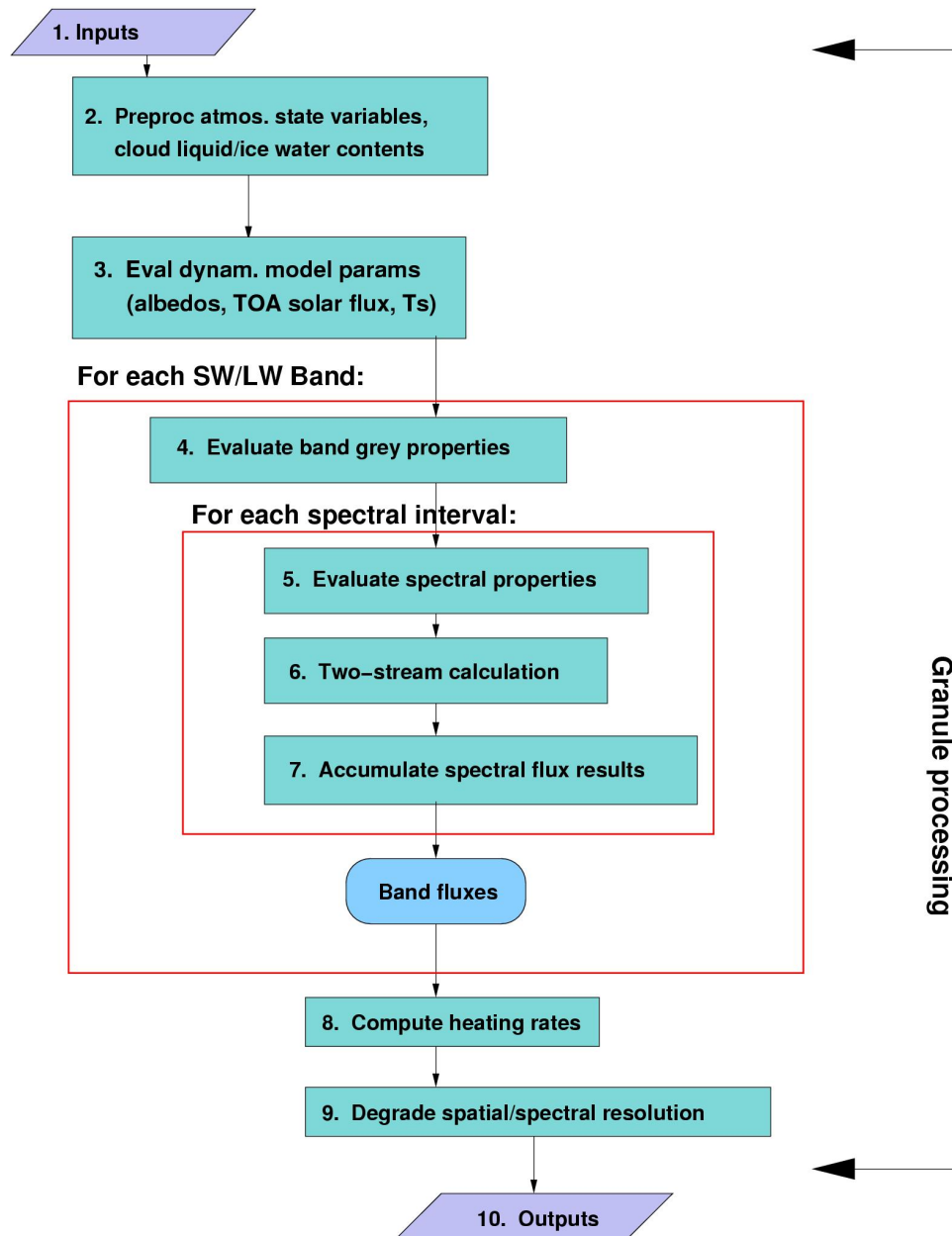


Figure 1: Flow diagram of the steps in the execution of the 2B-FLXHR algorithm.

2.2.3 Implementation

The CloudSat 2B-FLXHR algorithm is only run if the 2B-CWC product is available and passes its internal quality control (QC) criteria. Some specific features of the implementation are summarized as follows:

1. The top boundary condition (top of atmosphere) consists of zero downwelling longwave flux and a nonzero downwelling solar flux adjusted for the eccentricity of the earth's orbit.
2. The lower boundary condition (bottom of atmosphere) for longwave calculation is an upwelling flux from the surface

based on the surface temperature and an emissivity of 1.0 (i.e. black within each band). The lower boundary condition for each shortwave calculation assumes the surface behaves as a lambertian reflector. The algorithm is implemented such that one albedo may be used for the visible bands, another used for all near-IR bands.

3. Aerosols are presently excluded, although appropriate routines are included in the 2B-FLXHR algorithm such that aerosols could be included if appropriate data became available.
4. Cloud liquid and ice water are assumed to be uniformly distributed in layers where cloud is present (no fractional cloudiness).
5. Cloud water content is partitioned into liquid and ice following the ice fraction prescribed by the 2B-CWC product.
6. Shortwave calculations are optimized so that flux calculations are only done for daylit columns.
7. Evaluations of Planck emission are done using a polynomial expression to improve speed.
8. Atmospheric profiles of water vapor, temperature, and Ozone in the algorithm are determined from ECMWF analyses (see below).
9. Uniform mixing ratios of CO_2 , CH_4 and N_2O are included with values of 360.0, 1.6, and 0.28 ppmv respectively.
10. At present 2B-FLXHR uses only the radar-only version of the 2B-CWC algorithm and does not, therefore, invoke optical depths from the 2B-TAU product.
11. In precipitation, where the 2B-CWC algorithm generally fails to converge, the 2B-FLXHR algorithm assumes a threshold value of 0.5 gm^{-3} for the water contents of all cloud filled bins according to 2B-GEOPROF. While this value does not rigorously derive from the observed reflectivities, it is large enough to saturate the LW and SW radiation in just a few bins. Thus the uncertainties introduced by this assumption are not likely to be prohibitively large.
12. After processing each orbit, 2B-FLXHR will also routinely compute top of the atmosphere (TOA) and surface (SFC) flux statistics for quality assessment purposes (see Section 7 for details).

3 Algorithm Inputs

3.1 CloudSat Level 2 Products

Time and location for each CloudSat pixel are supplied by the CloudSat geometric profile product (2B-GEOPROF). Table 2 summarizes the appropriate variables and their properties (see Li and Durden [9] for more details).

Table 2: Inputs from 2B-GEOPROF (per profile)

| Variable Name | Dimensions | Range | Units | Description |
|---------------------|--------------|---------------------|-------|--|
| <i>TAI_start</i> | scalar | 0 - 6×10^8 | s | International Atomic Time at granule start |
| <i>Profile_time</i> | scalar | 0 - 86400 | s | elapsed time since <i>TAI_start</i> |
| <i>ray_lat</i> | scalar | -90 - +90 | deg | latitude |
| <i>ray_lon</i> | scalar | -180 - +180 | deg | longitude |
| <i>Height</i> | vector (125) | -5000 - 30000 | m | Height of each range bin |
| <i>nSurfaceBin</i> | scalar | 1 - nbin | - | surface bin number |

The 2B-FLXHR algorithm also requires as input complete profiles of cloud liquid water content and ice water content from the 2B-CWC product. At present only the radar-only estimates are required along with appropriate quality control flags. 2B-CWC also implicitly determines the vertical sampling interval for the output. A detailed description of these products and their sizes is provided in Table 3.

Table 3: Inputs from 2B_CWC (per profile)

| Variable Name | Dimensions | Range | Units | Description |
|------------------|--------------|----------|-------------------|--|
| <i>ro_lwc</i> | vector (125) | 0 - 10 | g/m ³ | radar-only cloud liquid water content |
| <i>ro_iwc</i> | vector (125) | 0 - 1000 | mg/m ³ | radar-only cloud ice water content |
| <i>ro_lre</i> | vector (125) | 0 - 1000 | mg/m ³ | radar-only liquid cloud effective radius |
| <i>ro_ire</i> | vector (125) | 0 - 1000 | mg/m ³ | radar-only ice cloud effective radius |
| <i>icefrac</i> | scalar | 0 - 1 | – | Ice phase fraction |
| <i>ro_status</i> | scalar | 0 - 20 | – | Radar-only status flag |

3.2 Ancillary Data Sets

3.2.1 Atmospheric State Variables

Atmospheric state variables describing the background atmospheric and surface properties are supplied to 2B-FLXHR by the CloudSat ECMWF-AUX data product. The ECMWF-AUX inputs required for 2B-FLXHR consist of surface pressure, surface temperature, profiles of pressure, temperature, and specific humidity and are summarized in Table 4.

Table 4: Inputs from ECMWF-AUX (per profile)

| Variable Name | Dimensions | Range | Units | Description |
|---------------|--------------|------------------------|-------|---------------------|
| T_{sfc} | scalar | 150-350 | K | surface temperature |
| P | vector (125) | 0 - 1.02×10^5 | Pa | pressure |
| T | vector (125) | 150-350 | K | temperature |
| q_v | vector (125) | 0.00 - 1.00 | kg/kg | specific humidity |
| O_3 | vector (125) | 0-??? | ppm | Ozone mixing ratio |

3.2.2 CloudSat Ancillary Albedo Dataset

In addition to the products listed above, the flux calculations in 2B-FLXHR require the reflection properties of the underlying surface to be specified. For this purpose, 2B-FLXHR requires surface albedo estimates in the visible and near-infrared spectral bands from the CloudSat ancillary albedo product, AN-ALBEDO. Table 5 summarizes the variables required.

Table 5: Inputs from AN-ALBEDO (per profile)

| Variable Name | Dimensions | Range | Units | Description |
|---------------|------------|---------|-------|------------------------|
| $A_{s,v}$ | scalar | 0. - 1. | – | visible surface albedo |
| $A_{s,nir}$ | scalar | 0. - 1. | – | near-IR surface albedo |

3.2.3 Ancillary MODIS Data

The only additional ancillary data currently required by 2B-FLXHR is the solar zenith angle supplied by the MODIS-AUX data product. Details concerning the MODIS-AUX solar zenith angle are summarized in Table 6.

Table 6: Algorithm Parameters (per profile)

| Variable Name | Dimensions | Range | Units | Description |
|---------------|------------|-----------|---------|--------------------|
| SZA | scalar | 0. - 180. | degrees | solar zenith angle |

3.3 Control and Calibration

At present no calibration of the 2B-FLXHR algorithm is planned. As a result, no ancillary control or calibration data is required. See Section 4.3.2 for details regarding planned validation activities for 2B-FLXHR products.

4 Algorithm Summary

4.1 Pseudo-code

The following provides a pseudo-code description outlining the details of the steps in the algorithm flow diagram in Figure 1:

```

start 2B-FLXHR
open 2B-GEOPROF
open 2B-CWC
open ECMWF-AUX
open 2B-FLXHR output file
open albedo ancillary data file (AN-ALBEDO)
set top-of-atmosphere, beam-normal irradiance  $F_0$ 
for-each profile
    read ray number  $r$  (2B-GEOPROF)
    get time  $t$  (2B-GEOPROF)
    get geometry parameters  $lat, nSurfaceBin$  (2B-GEOPROF)
    compute solar zenith angle ( $SZA$ ), orbital eccentricity factor
    read cloud liquid and ice water contents (2B-CWC)
    read atmosphere state variables (ECMWF-AUX)
    read surface albedos (AN-ALBEDO)
    compute fluxes and heating rates
end-for-each profile
compute scale factors, offsets
compute scaled fluxes and heating rates
compute latitude-mean flux and heating rate statistics
write scale factors, offsets (2B-FLXHR)
write scaled fluxes, heating rates (2B-FLXHR)
write latitude-mean flux and heating rate statistics
close 2B-FLXHR output file
close AN-ALBEDO
close 2B-CWC
close ECMWF-AUX
close 2B-GEOPROF
stop 2B-FLXHR

```

4.2 Algorithm Parameters

In addition to the input variables listed in Section 3, a number of parameters are set in the 2B-FLXHR algorithm itself. These are summarized in Table 7.

Table 7: Algorithm Parameters (per profile)

| Variable Name | Dimensions | Range | Units | Description |
|---------------|------------|-------------|---------------------|--|
| F_0 | scalar | 1500 | $Wm^{-2}\mu m^{-1}$ | TOA incident, beam-normal irradiance |
| e | scalar | 0. - 1. | – | orbital eccentricity factor |
| rel | scalar | 10. | μm | liquid cloud effective radius ¹ |
| rei | scalar | 30. | μm | ice cloud effective radius ¹ |
| $wpfill$ | scalar | 0.5 | kgm^3 | water path fill value ² |
| $[CO_2]$ | scalar | 300. - 400. | ppmv | carbon dioxide concentration |
| $[CH_4]$ | scalar | TBD | ppmv | methane concentration |
| $[N_2O]$ | scalar | TBD | ppmv | nitrous oxide concentration |

4.3 Algorithm Performance

4.3.1 Timing Requirements and Performance

As retrievals are to be performed in real time, the requirement on the computational speed of the algorithm is estimated from the following considerations:

- satellite speed along ground track $\sim 7 \text{ km s}^{-1}$
- 3.5 km resolution along-track

This yields approximately two pixels to process per second allowing a half second per pixel, in the absence of additional constraints. However, since the algorithm requires inputs from a number of other CloudSat products to run their processing time must be factored in to the calculation. Based on estimates of the processing times for the 2B-GEOPROF and 2B-CWC algorithms, we impose a maximum processing time of 0.05-0.1 seconds per ray.

4.3.2 Uncertainty Requirements and Performance

The specific goals for the quality of the 2B-FLXHR flux and heating rate products as laid out in the CloudSat Step-2 ESSP-2 Proposal are as follows:

- Atmospheric fluxes at 500m resolution accurate to 5 Wm^{-2} .
- Atmospheric heating rates at 500m resolution accurate to 1 Kday^{-1} .

The evaluation of 2B-FLXHR products in the context of these goals can be considered as a two-pronged approach consisting of both verification of the inputs to the algorithm as well as more traditional validation of the output. This approach not only evaluates the performance of the algorithm for comparison to the mission requirements but also provides a unique opportunity to study the contributions of various sources of error to the overall uncertainty in the product.

The verification of algorithm inputs is largely covered as part of the validation plans for the other CloudSat products up the level 2 chain. Uncertainties in the 2B-CWC products, for example, will be provided by their respective algorithm teams after launch and the uncertainties in the atmospheric state variables from the ECMWF-AUX and AN-ALBEDO datasets will be obtained from their sources. Using these error estimates, a series of sensitivity studies will be conducted using an offline version of 2B-FLXHR algorithm and a subset of the CloudSat observations. The results will provide bounds on the expected uncertainties in the flux and heating rate products due to errors in all algorithm inputs and will serve as an initial evaluation of algorithm performance.

To supplement these sensitivity studies, flux observations/estimates from the Clouds and the Earth's Radiant Energy System (CERES) aboard Aqua will also be compared with the 2B-FLXHR products. The CERES instrument provides estimates of outgoing longwave and shortwave radiation at the top of the atmosphere and, through independent algorithms, the CERES team infer longwave and shortwave fluxes at the Earth's surface. Both will be compared with CloudSat products

on a range of temporal and spatial scales. While these comparisons are restricted to fluxes at the atmospheric boundaries (i.e. the top of the atmosphere and the surface) they will serve to verify the uncertainty estimates derived through the above sensitivity studies providing a more complete analysis of the algorithm's performance characteristics. A combination of the results obtained from each of these evaluation approaches will ultimately be compared to the requirements above to assess its overall performance in the context of the mission as a whole.

5 Data Product Output Format

5.1 Data Contents

To reiterate, the 2B-FLXHR algorithm generates estimates of upwelling and downwelling longwave and shortwave radiative fluxes as well as longwave and shortwave radiative heating at the CPR resolution. Each pixel is also assigned two distinct status flags providing additional information pertaining to the output.

The RVOD status flag indicates whether or not the CWC products used in the given pixel were constrained using visible optical depth information from CloudSat's 2B-TAU product. Also, noting that different algorithms may be used to produce the 2B-CWC inputs for daytime and nighttime pixels, the status flag will indicate whether the pixel was observed during the day or at night. Possible values for this flag are summarized in Table 9.

Table 8: Values for RVOD status flag.

| Value | Meaning |
|-------|--|
| 01 | Daytime clear pixel |
| 02 | Nighttime clear pixel |
| 03 | Daytime pixel with valid optical depth information (2B-CWC-RVOD) |
| 04 | Nighttime pixel with valid optical depth information (2B-CWC-RVOD) |
| 05 | Daytime radar-only (2B-CWC-RO) pixel |
| 06 | Nighttime radar-only (2B-CWC-RO) pixel |

Each pixel will also be assigned a status flag with a value between 1 and 20 that will identify the cloud type or types present in the scene as well as indicating scenes in which drizzle may have contaminated the 2B-CWC product. Table 9 provides a summary of all status flags used by 2B-FLXHR. Note that all pixels with flag values of eight or less should contain valid flux and heating rate output while flags greater than this value will generally be filled with missing values. Flags 5-7 are all indicative of possible precipitation within the CloudSat footprint. In cases where the CWC algorithm was able to converge on a solution, it was used to specify liquid and ice water contents. Flag values of 6 or 7 indicate cases where the CWC liquid or ice water content algorithms failed, respectively, and fill values were assumed for the appropriate water contents (see step 11 in Section 2.2.2).

Table 9: Values for flux and heating rate status flag.

| Value | Meaning |
|-------|---|
| 01 | Clear pixel |
| 02 | Only a liquid cloud present |
| 03 | Only an ice cloud present |
| 04 | Both types of non-precipitating cloud present |
| 05 | Possible drizzle/precipitation |
| 06 | Filled LWC in precipitation |
| 07 | Filled IWC in precipitation |
| 08 | High χ^2 in either LWC or IWC retrieval |
| 09 | Bad LWC input data (see 2B-CWC for explanation) |
| 10 | Bad IWC input data (see 2B-CWC for explanation) |
| 17 | Bad surface bin in 2B-GEOPROF |
| 18 | Bad MODIS-AUX input data |
| 19 | Out-of-bounds flux encountered |

Among the expected uses for CloudSat flux and heating rate data is to provide a source of information for analyzing global and regional radiation budgets. To this end, 2B-FLXHR will also provide mean fluxes at the top of the atmosphere (TOA) and surface (SFC) and mean column-integrated radiative heating rates spatially averaged over both the full CloudSat domain and various latitude belts ranging from the tropics to the high latitudes. The particular latitude belts chosen for 2B-FLXHR and appropriate physical interpretations are summarized in Table 10. For each of these regions, 2B-FLXHR

Table 10: Latitude ranges over which statistics will be computed.

| Name | Range |
|----------------------|---------------------------|
| Orbit | The entire CloudSat orbit |
| North High Latitudes | 55 N to 90 N |
| North Midlatitudes | 35 N to 55 N |
| North Subtropics | 23.5 N to 35 N |
| Tropics | 23.5 S to 23.5 N |
| South Subtropics | 23.5 S to 35 S |
| South Midlatitudes | 35 S to 55 S |
| South High Latitudes | 55 S to 90 S |

will provide the mean and standard deviation of upwelling and downwelling longwave and shortwave fluxes at both TOA and SFC over each orbit. The mean and standard deviation of the estimated column-integrated longwave and shortwave radiative heating will also be computed and stored.

All of these 2B-FLXHR data products are summarized in Table 11. The parameter “nz” is the total number of vertical intervals at which data are reported, typically 125, and the parameter “nb” is the number of bands for which data are reported, in this case two. “nray” is the total number of profiles in the data granule, “nflags” is the total number of pixel status flags that may be assigned, and “nlatbins” is the number of latitude bins for which TOA and SFC flux statistics are produced.

5.2 Data Format Overview

In addition to the data specific to the 2B-FLXHR algorithm results, the HDF-EOS data structure may incorporate granule data/metadata (describing the characteristics of the orbit or granule) and supplementary ray data/metadata. The data structure is described in Table 12. Only those data fields specifically required by the 2B-FLXHR algorithm are listed in the table and included in the descriptions in Section 5.3. The entries in the “Size” column of the table represent the array size where appropriate (*e.g.*, nray), the variable type (REAL, INTEGER, CHAR) and the size in bytes of each element (*e.g.*, (4)). The parameter “nray” is the total number of profiles in the granule.

5.3 Data Descriptions

2B-FLXHR data fields:

$FD_{\lambda z}$ (SDS, nz*nb*nray*INTEGER(2))

Band-integrated downwelling flux profile estimates. Shortwave estimates are stored as the first element followed by the longwave estimates. All values range from 0 to 1500 and are stored as two-byte integers with no scaling. The fill value -999 corresponds to bad/missing input or out-of-bounds fluxes.

$FDclr_{\lambda z}$ (SDS, nz*nb*nray*INTEGER(2))

Band-integrated downwelling flux profile estimates for cloud-cleared skies. These estimates assume identical atmospheric and surface properties as $FD_{\lambda z}$ but all cloud water contents are set to zero. Shortwave estimates are stored as the first element followed by the longwave estimates. All values range from 0 to 1500 and are stored as two-byte integers with no scaling. The fill value -999 corresponds to bad/missing input or out-of-bounds fluxes.

$FU_{\lambda z}$ (SDS, nz*nb*nray*INTEGER(2))

Band-integrated upwelling flux profile estimates. Shortwave estimates are stored as the first element followed by the longwave estimates. All values range from 0 to 1500 and are stored as two-byte integers with no scaling. The fill value -999 corresponds to bad/missing input or out-of-bounds fluxes.

Table 11: Algorithm Outputs

| Variable Name | Dimensions | Range | Units | Description |
|---------------------|------------------------|--------------|--------------|---|
| $FD_{\lambda,z}$ | nray*nz*nb vector | 0 - 1500. | Wm^{-2} | downwelling flux |
| $FDclr_{\lambda,z}$ | nray*nz*nb vector | 0 - 1500. | Wm^{-2} | downwelling flux in cleared-skies |
| $FU_{\lambda,z}$ | nray*nz*nb vector | 0 - 1500. | Wm^{-2} | upwelling flux |
| $FUclr_{\lambda,z}$ | nray*nz*nb vector | 0 - 1500. | Wm^{-2} | upwelling flux in cleared-skies |
| $TOACRE_{\lambda}$ | nray*nb vector | 0 - 1500. | Wm^{-2} | Top-of-atmosphere cloud radiative effect |
| $BOACRE_{\lambda}$ | nray*nb vector | 0 - 1500. | Wm^{-2} | Bottom-of-atmosphere cloud radiative effect |
| $QR_{\lambda,z}$ | nray*nz*(nb-1) vector | -200. - 200. | $K day^{-1}$ | heating rate |
| RVOD Status | nray scalar | 1 - 6 | - | RVOD status flag |
| Status | nray scalar | 1 - 20 | - | pixel status flag |
| BinCounts | nflags*nlatbins vector | 0 - nray | - | Number of pixels in each lat/status bin |
| Meansolar | nflags*nlatbins vector | 0 - 1500 | Wm^{-2} | mean solar insolation |
| Sigmasolar | nflags*nlatbins vector | 0 - 1500 | Wm^{-2} | standard deviation of solar insolation |
| MeanOSR | nflags*nlatbins vector | 0 - 1500 | Wm^{-2} | mean OSR |
| SigmaOSR | nflags*nlatbins vector | 0 - 1500 | Wm^{-2} | standard deviation of OSR |
| MeanSSR | nflags*nlatbins vector | 0 - 1500 | Wm^{-2} | mean SSR |
| SigmaSSR | nflags*nlatbins vector | 0 - 1500 | Wm^{-2} | standard deviation of SSR |
| MeanSFCR | nflags*nlatbins vector | 0 - 1500 | Wm^{-2} | mean surface reflection |
| SigmaSFCR | nflags*nlatbins vector | 0 - 1500 | Wm^{-2} | standard deviation of surface reflection |
| MeanOLR | nflags*nlatbins vector | 0 - 1500 | Wm^{-2} | mean OLR |
| SigmaOLR | nflags*nlatbins vector | 0 - 1500 | Wm^{-2} | standard deviation of OLR |
| MeanSLR | nflags*nlatbins vector | 0 - 1500 | Wm^{-2} | mean SLR |
| SigmaSLR | nflags*nlatbins vector | 0 - 1500 | Wm^{-2} | standard deviation of SLR |
| MeanSFCE | nflags*nlatbins vector | 0 - 1500 | Wm^{-2} | mean surface emission |
| SigmaSFCE | nflags*nlatbins vector | 0 - 1500 | Wm^{-2} | standard deviation of surface emission |
| MeanQLW | nflags*nlatbins vector | -10 - 10 | $K day^{-1}$ | mean atmospheric longwave heating |
| SigmaQLW | nflags*nlatbins vector | -10 - 10 | $K day^{-1}$ | standard deviation of atmospheric longwave heating |
| MeanQSW | nflags*nlatbins vector | -10 - 10 | $K day^{-1}$ | mean atmospheric shortwave heating |
| SigmaQSW | nflags*nlatbins vector | -10 - 10 | $K day^{-1}$ | standard deviation of atmospheric shortwave heating |

 $FUclr_{\lambda,z}$ (SDS, nz*nb*nray*INTEGER(2))

Band-integrated upwelling flux profile estimates for cloud-cleared skies. These estimates assume identical atmospheric and surface properties as $FD_{\lambda,z}$ but all cloud water contents are set to zero. Shortwave estimates are stored as the first element followed by the longwave estimates. All values range from 0 to 1500 and are stored as two-byte integers with no scaling. The fill value -999 corresponds to bad/missing input or out-of-bounds fluxes.

 $QR_{\lambda,z}$ (SDS, nz*nb*nray*INTEGER(2))

Band-integrated heating rate estimates. Shortwave estimates are stored as the first element followed by the longwave estimates. All values are multiplied by 100 and stored as two-byte integers. Prior to adjustment all values fall between -200 and 200 $K d^{-1}$. The fill value -999 corresponds to bad/missing input or out-of-bounds fluxes.

 $TOACRE_{\lambda}$ (SDS, nray*INTEGER(2))

Top of the atmosphere cloud radiative effect (also referred to as cloud 'forcing'). Shortwave estimates are stored as the first element followed by the longwave estimates. All values range from 0 to 1500 and are stored as two-byte integers.

 $BOACRE_{\lambda}$ (SDS, nray*INTEGER(2))

Bottom of the atmosphere (i.e. surface) cloud radiative effect (also referred to as cloud 'forcing'). Shortwave estimates are stored as the first element followed by the longwave estimates. All values range from 0 to 1500 and are stored as two-byte integers.

RVOD_status_flg (SDS, nray*INTEGER(2))

Table 12: HDF-EOS File Structure

| Structure/Data Name | | | Size | |
|---------------------|----------------------------|---------------------|-------------------------------|----------------------------|
| Data Granule | Swath Metadata | Common metadata | TBD | TBD |
| | | 2B-FLXHR metadata | $F_{\lambda z}$ scale factor | REAL(4) |
| | | | $F_{\lambda z}$ offset | REAL(4) |
| | | | $QR_{\lambda z}$ scale factor | REAL(4) |
| | | | $QR_{\lambda z}$ offset | REAL(4) |
| | | | BF scale factor | REAL(4) |
| | | | BF offset | REAL(4) |
| | | | BQR scale factor | REAL(4) |
| | | | BQR offset | REAL(4) |
| | Flag counts | nflags*INT(2) | | |
| | Swath | Common data fields | Time | nray*REAL(8) |
| | | | Status flag | nray*INTEGER(2) |
| | | | Geolocation latitude | nray*REAL(4) |
| | | | Surface bin number | nray*INT(2) |
| | | 2B-FLXHR pixel data | $FD_{\lambda z}$ | nz*nb*nray*INTEGER(2) |
| | | | $FDclr_{\lambda z}$ | nz*nb*nray*INTEGER(2) |
| | | | $FU_{\lambda z}$ | nz*nb*nray*INTEGER(2) |
| | | | $FUclr_{\lambda z}$ | nz*nb*nray*INTEGER(2) |
| | | | $QR_{\lambda z}$ | nz*(nb-1)*nray*INTEGER(2) |
| | | | TOACRE | nray*INTEGER(2) |
| | | | BOACRE | nray*INTEGER(2) |
| | | | RVOD_status_fxhr | nray*INTEGER(2) |
| | | 2B-FLXHR orbit data | BinCounts | nlatbins*nflags*INTEGER(2) |
| | | | Meansolar | nlatbins*nflags*INTEGER(2) |
| | | | Sigmasolar | nlatbins*nflags*INTEGER(2) |
| | MeanOSR | | nlatbins*nflags*INTEGER(2) | |
| | SigmaOSR | | nlatbins*nflags*INTEGER(2) | |
| | MeanSSR | | nlatbins*nflags*INTEGER(2) | |
| | SigmaSSR | | nlatbins*nflags*INTEGER(2) | |
| | MeanSFCR | | nlatbins*nflags*INTEGER(2) | |
| | SigmaSFCR | | nlatbins*nflags*INTEGER(2) | |
| | MeanOLR | | nlatbins*nflags*INTEGER(2) | |
| | SigmaOLR | | nlatbins*nflags*INTEGER(2) | |
| MeanSLR | nlatbins*nflags*INTEGER(2) | | | |
| SigmaSLR | nlatbins*nflags*INTEGER(2) | | | |
| MeanSFCE | nlatbins*nflags*INTEGER(2) | | | |
| SigmaSFCE | nlatbins*nflags*INTEGER(2) | | | |
| MeanQSW | nlatbins*nflags*INTEGER(2) | | | |
| SigmaQSW | nlatbins*nflags*INTEGER(2) | | | |
| MeanQLW | nlatbins*nflags*INTEGER(2) | | | |
| SigmaQLW | nlatbins*nflags*INTEGER(2) | | | |

A two-byte integer flag with bits allocated according to Table 8. This flag includes indicators of the presence of clouds, optical depth information, and whether the pixel was observed during the day or at night.

Status (SDS, nray*INTEGER(2))

A two-byte integer quality control flag with bits allocated according to Table 9. This flag includes indicators of bad input data, bad flux data, drizzle, etc.

BinCounts (SDS, nlatbins*nflags*INTEGER(2))

Number of pixels in orbit accumulated in each latitude band and status flag bin. All values range from 0 to “nray” and are stored as two-byte integers. The latitude bands over which statistics will be compiled are

summarized in Table 10.

Meansolar (SDS, nlatbins*nflags*INTEGER(2))

Mean downwelling shortwave flux at the top of the atmosphere over each latitude band and status flag bin. All values range from 0 to 1500 and are stored as two-byte integers. The latitude bands over which statistics will be computed are summarized in Table 10.

Sigmasolar (SDS, nlatbins*nflags*INTEGER(2))

Standard deviation of downwelling shortwave flux at the surface over each latitude band and status flag bin. All values range from 0 to 1500 and are stored as two-byte integers. The latitude bands over which statistics will be computed are summarized in Table 10.

MeanOSR (SDS, nlatbins*nflags*INTEGER(2))

Mean upwelling shortwave flux at the top of the atmosphere, or outgoing shortwave radiation (OSR), over each latitude band and status flag bin. All values range from 0 to 1500 and are stored as two-byte integers. The latitude bands over which statistics will be computed are summarized in Table 10.

SigmaOSR (SDS, nlatbins*nflags*INTEGER(2))

Standard deviation of upwelling shortwave flux at the top of the atmosphere, or outgoing shortwave radiation (OSR), over each latitude band and status flag bin. All values range from 0 to 1500 and are stored as two-byte integers. The latitude bands over which statistics will be computed are summarized in Table 10.

MeanSSR (SDS, nlatbins*nflags*INTEGER(2))

Mean downwelling shortwave flux at the surface, or surface shortwave radiation (SSR), over each latitude band and status flag bin. All values range from 0 to 1500 and are stored as two-byte integers. The latitude bands over which statistics will be computed are summarized in Table 10.

SigmaSSR (SDS, nlatbins*nflags*INTEGER(2))

Standard deviation of downwelling shortwave flux at the surface, or surface shortwave radiation (SSR), over each latitude band and status flag bin. All values range from 0 to 1500 and are stored as two-byte integers. The latitude bands over which statistics will be computed are summarized in Table 10.

MeanSFCR (SDS, nlatbins*nflags*INTEGER(2))

Mean upwelling, or reflected, shortwave flux at the surface over each latitude band and status flag bin. All values range from 0 to 1500 and are stored as two-byte integers. The latitude bands over which statistics will be computed are summarized in Table 10.

SigmaSFCR (SDS, nlatbins*nflags*INTEGER(2))

Standard deviation of upwelling, or reflected, shortwave flux at the surface over each latitude band and status flag bin. All values range from 0 to 1500 and are stored as two-byte integers. The latitude bands over which statistics will be computed are summarized in Table 10.

MeanOLR (SDS, nlatbins*nflags*INTEGER(2))

Mean upwelling longwave flux at the top of the atmosphere, or outgoing longwave radiation (OLR), over each latitude band and status flag bin. All values range from 0 to 1500 and are stored as two-byte integers. The latitude bands over which statistics will be computed are summarized in Table 10.

SigmaOLR (SDS, nlatbins*nflags*INTEGER(2))

Standard deviation of upwelling longwave flux at the top of the atmosphere, or outgoing longwave radiation (OLR), over each latitude band and status flag bin. All values range from 0 to 1500 and are stored as two-byte integers. The latitude bands over which statistics will be computed are summarized in Table 10.

MeanSLR (SDS, nlatbins*nflags*INTEGER(2))

Mean downwelling longwave flux at the surface, or surface longwave radiation (SLR), over each latitude band and status flag bin. All values range from 0 to 1500 and are stored as two-byte integers. The latitude bands over which statistics will be computed are summarized in Table 10.

SigmaSLR (SDS, nlatbins*nflags*INTEGER(2))

Standard deviation of downwelling longwave flux at the surface, or surface longwave radiation (SLR), over each latitude band and status flag bin. All values range from 0 to 1500 and are stored as two-byte integers. The latitude bands over which statistics will be computed are summarized in Table 10.

MeanSFCE (SDS, nlatbins*nflags*INTEGER(2))

Mean upwelling, or emitted, longwave flux at the surface over each latitude band and status flag bin. All values range from 0 to 1500 and are stored as two-byte integers. The latitude bands over which statistics will be computed are summarized in Table 10.

SigmaSFCE (SDS, nlatbins*nflags*INTEGER(2))

Standard deviation of upwelling, or emitted, longwave flux at the surface over each latitude band and status flag bin. All values range from 0 to 1500 and are stored as two-byte integers. The latitude bands over which statistics will be computed are summarized in Table 10.

MeanQSW (SDS, nlatbins*nflags*INTEGER(2))

Mean total atmospheric shortwave heating over each latitude band and status flag bin. All values are multiplied by 100 and stored as two-byte integers. Prior to adjustment all values range from -10 to 10. The latitude bands over which statistics will be computed are summarized in Table 10.

SigmaQSW (SDS, nlatbins*nflags*INTEGER(2))

Standard deviation of total atmospheric shortwave heating over each latitude band and status flag bin. All values are multiplied by 100 and stored as two-byte integers. Prior to adjustment, all values range from -10 to 10. The latitude bands over which statistics will be computed are summarized in Table 10.

MeanQLW (SDS, nlatbins*nflags*INTEGER(2))

Mean total atmospheric longwave heating over each latitude band and status flag bin. All values are multiplied by 100 and stored as two-byte integers. Prior to adjustment, all values range from -10 to 10. The latitude bands over which statistics will be computed are summarized in Table 10.

SigmaQLW (SDS, nlatbins*nflags*INTEGER(2))

Standard deviation of total atmospheric longwave heating over each latitude band and status flag bin. All values are multiplied by 100 and stored as two-byte integers. Prior to adjustment, all values range from -10 to 10. The latitude bands over which statistics will be computed are summarized in Table 10.

2B-FLXHR metadata fields: **$F_{\lambda z}$ scale factor** (SDS attribute, REAL(4))

Scale factor used to rescale pixel-level fluxes, $FU_{\lambda z}$, $FD_{\lambda z}$, $FU_{clr_{\lambda z}}$, and $FD_{clr_{\lambda z}}$ as well as cloud forcings $TOACRE_{\lambda}$ and $BOACRE_{\lambda}$.

 $F_{\lambda z}$ offset (SDS attribute, REAL(4))

Offset added to pixel-level fluxes, $FU_{\lambda z}$, $FD_{\lambda z}$, $FU_{clr_{\lambda z}}$, and $FD_{clr_{\lambda z}}$ as well as cloud forcings $TOACRE_{\lambda}$ and $BOACRE_{\lambda}$.

 $QR_{\lambda z}$ scale factor (SDS attribute, REAL(4))

Scale factor used to rescale pixel-level radiative heating rates.

 $QR_{\lambda z}$ offset (SDS attribute, REAL(4))

Offset added to pixel-level radiative heating rates.

BF scale factor (SDS attribute, REAL(4))

Scale factor used to rescale bin-mean (and standard deviation) fluxes.

BF offset (SDS attribute, REAL(4))

Offset added to bin-mean (and standard deviation) fluxes.

BQR scale factor (SDS attribute, REAL(4))

Scale factor used to rescale bin-mean (and standard deviation) radiative heating rates.

BQR offset (SDS attribute, REAL(4))

Offset added to bin-mean (and standard deviation) radiative heating rates.

Flag counts (SDS attribute, nflags*INT(2))

Granule status flag statistics providing the number of pixels along the orbit that are assigned each of the values described in Table 9 in the form of a 2-byte integer.

Common data fields:**time** (nray*REAL(8))

Frame (or ray) international atomic time. Seconds since 00:00:00 1 Jan 1993.

geolocation latitude (nray*REAL(4))

The latitude of the center of the IFOV at the altitude of the earth ellipsoid (Li and Durden [9]).

Surface bin number (nray*INT(2))

Index of radar range bin coincident with earth' surface.

Common metadata fields:

No additional metadata are specifically required by the 2B-FLXHR algorithm.

6 Example

Sample heating rates from the 2B-FLXHR product for a small segment of CloudSat orbit 702 are presented in Figure 3. Selected input fields from 2B-GEOPROF and 2B-CWC for the same orbit segment are given in Figure 3 for comparison.

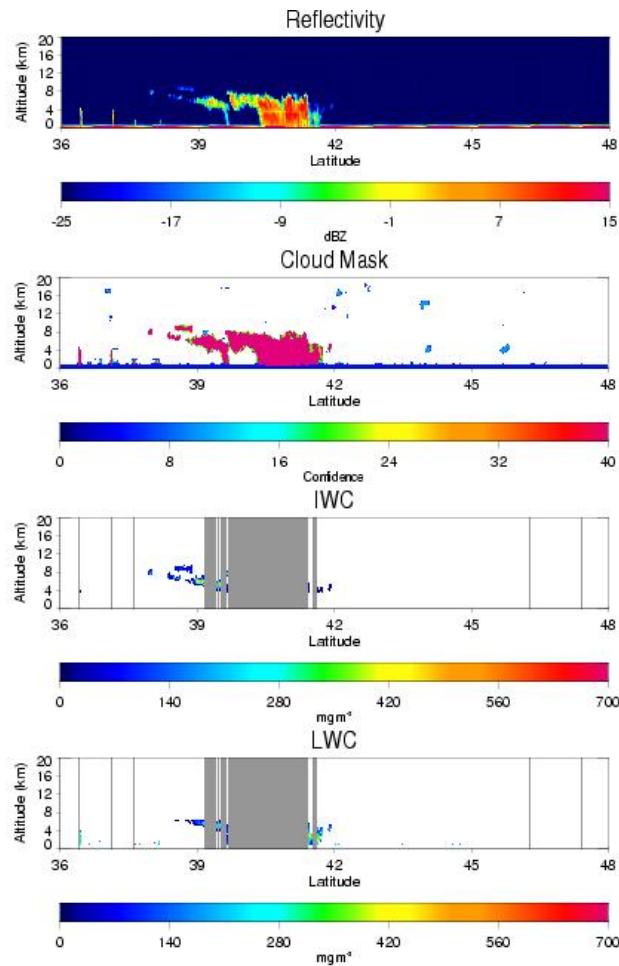


Figure 2: Inputs to 2B-FLXHR from a portion of granule 00702 between 36 and 48°N. Observed reflectivities and the 2B-GEOPROF cloud mask are shown in the upper two panels while the lower two show retrieved IWC and LWC from the 2B-CWC product.

This section of orbit illustrates a number of important aspects of the 2B-FLXHR algorithm. First, note that the vertical gray bars on Figure 2 correspond to regions for which the 2B-CWC algorithm failed to converge, generally as a result of precipitation in the satellites FOV. As noted in Section 2.2.3, these profiles are modeled by assuming a threshold water content of 0.5 gm^{-3} in any bin that is indicated as being cloudy according to the 2B-GEOPROF product. Thus almost all of these regions are filled in the corresponding 2B-FLXHR heating fields shown in Figure 3 and the apparent continuity in these fields lend support to the validity of this approximation in lieu of a more rigorous precipitation product. The single

bar that remains (near 47.5°N) represents a series of profiles for which no data could be produced due to missing solar-zenith angle input from MODIS-AUX. While the occurrence of such pixels is generally infrequent and almost exclusively limited to the early off-nadir period of the mission, they illustrate the importance of using the status flag supplied with every 2B-FLXHR profile to identify potential bad data.

Qualitative inspection of the remainder of the scene illustrates many features commonly found in a typical 2B-FLXHR granule. The most interesting of these is the precipitating cloud system between 39 and 42°N that demonstrates a narrow layer of LW cloud top cooling followed by a deeper layer of warming resulting from the deeper penetration of SW radiation into the cloud. South of 40.5°N , LW warming at cloud base is also evident outside the region where precipitation extends to the surface. In the clear-sky regions LW cooling generally dominates the middle atmosphere while a ubiquitous layer of stratospheric heating exists above 15 km. In the lowest few km, SW heating generally dominates due to the relatively strong incident solar flux at the 1:30pm local overpass time.

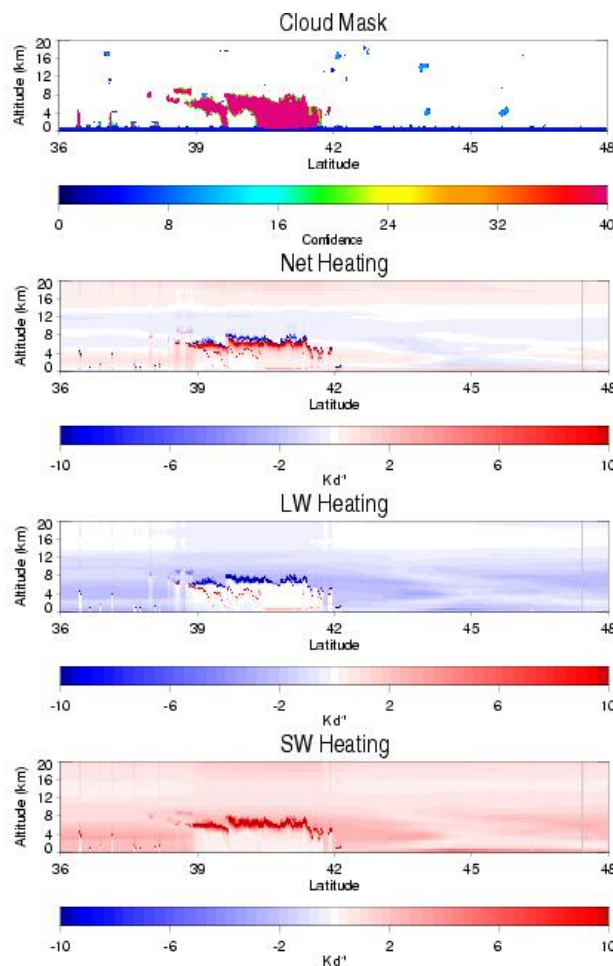


Figure 3: 2B-FLXHR output corresponding to the input shown in Figure 2. The 2B-GEOPROF cloud mask is repeated in the upper panel for reference while the remaining panels show vertical cross-sections of Net, LW and SW radiative heating rates, respectively.

7 Operator Instructions

The 2B-FLXHR algorithm is implemented in concert with the other level 2 algorithms as a component in the CloudSat Operational and Research Environment (CORE). As the final link in CloudSat's Level 2 product chain, 2B-FLXHR output is not directly used by any other algorithm but depends, either directly or indirectly, on almost all other level 2 products.

Thus 2B-FLXHR will only be run on pixels for which all other level 2 algorithms were successful. All other pixels will be flagged as missing data by assigning a value of -999 and skipped. Since this type of missing data is entirely based on prior products, it is assumed that any serious flaws in the processing chain owing to prior algorithms will have already been discovered. As a result no additional quality assessment is proposed regarding this type of missing data.

For all pixels with valid data in all other level 2 products, the quality of the 2B-FLXHR output will be evaluated on a pixel-by-pixel basis for unphysical flux estimates. Since the broadband radiative transfer model employed in the 2B-FLXHR algorithm has been extensively tested and is implemented in numerous other forms, its failure is unlikely and it is anticipated that the algorithm will produce reasonable output provided the appropriate 2B-LWC and 2B-IWC inputs are available. To ensure this is the case a simple threshold test will be employed. If any flux exceeds 1500 Wm^{-2} , all output for that pixel will be flagged as missing by assigning a value of -999. Likewise if any flux goes negative, all output data will be similarly flagged. These thresholds should never be exceeded even under unusual circumstances so, in the event that more than 10 such pixels occur within any orbit, a warning message will be relayed through the on-screen summary to alert the operator of a possible problem with the algorithm.

A second, more comprehensive quality assessment tool will be provided through a statistical summary of the 2B-FLXHR flux and heating rate estimates that will also be stored in the HDF-EOS output file for each orbit. Statistics regarding the number of breakdown of all CloudSat rays in each orbit into the output categories defined by the status flag (Table 9) will be stored in an additional metadata field called "Flag counts". In addition, mean and standard deviation statistics for fluxes at the atmospheric boundaries (top of the atmosphere and surface) will be computed for each value of the status flag over the latitude bands summarized in Table 10. These variables, stored as additional output data, will ordinarily be used to construct estimates of regional radiation budgets but can also be monitored by the operator to detect systematic variations in the algorithms performance with time and used by algorithm developers to trace the source of any errors that occur. A change of more than 25 % from one orbit to the next in any of the mean longwave flux estimates (MeanOLR, MeanSLR, MeanSFCE, or MeanQLW) is indicative of a potential problem with the algorithm

The final tool for quality assessment of the 2B-FLXHR product consists of a plot of the downwelling longwave flux over the entire orbit. The gross features in this plot should resemble those found in the other L2B products. In particular, the tops of clouds identified in the 2B-CLDCLASS product should be very well defined in the corresponding downwelling longwave flux field.

8 Changes Since Version 5.0

The primary changes to 2B-FLXHR for version 5.1 have centered on adapting to changes in the 2B-CWC algorithm and adding the capability to examine cloud impacts on radiative fluxes and heating rates. Specific changes include:

- The algorithm now explicitly incorporates effective radius information from the 2B-CWC product. This fixes a bug in Version 5 where the effective radii of liquid and ice clouds was set to climatological values.
- The interpretation of 2B-CWC flags has been improved leading to a significant reduction in the number of missing pixels in the output. A more comprehensive flagging system has been implemented to provide more detailed information regarding the input and characteristics of each pixel in the output (see Tables 8 and 9) and allow for the addition of the visible optical depth products in the next version of the algorithm.
- The product has been augmented with the addition of flux profile estimates for cloud-cleared pixels. Two sets of flux calculations are now reported for each pixel, one that represents the true state of the pixel consistent with the 2B-GEOPROF and 2B-CWC inputs and the other that corresponds to the same pixel with all clouds removed. This information can be used to assess the magnitude of cloud impacts on radiative heating on a pixel by pixel basis.
- Two additional fields are now reported that provide estimates of cloud radiative impacts on radiative fluxes at the top of the atmosphere and surface.
- The output format of heating rates has been modified slightly to fix a bug in the representation of missing values. Offsets are no longer added to these fields when they are stored.

9 Acronym List

CIRA Cooperative Institute for Research in the Atmosphere

CERES Clouds and the Earth's Radiant Energy System

CPR Cloud Profiling Radar

EOS Earth Observing System

HDF Hierarchical Data Format

IFOV Instantaneous Field of View

IWC Ice Water Content

LWC Liquid Water Content

MODIS Moderate Resolution Imaging Spectrometer

QC Quality Control

SDS Scientific Data Set

SFC Surface

TOA Top of Atmosphere

VTCW Vehicle Time Code Word

References

- [1] Stephens, G. L., P. M. Gabriel and P. T. Partain, 2001: "Parameterization of atmospheric radiative transfer. Part I: validity of simple models," *J. Atmos. Sci.*, 48, 3391 - 3409.
- [2] Stephens, G. L. and P. J. Webster, 1981: "Clouds and climate: Sensitivity of simple systems," *J. Atmos. Sci.*, 38, 235-247.
- [3] Fu, Q. and K. N. Liou, 1992: "On the correlated k-distribution method for radiative transfer in nonhomogeneous atmospheres," *J. Atmos. Sci.*, 49, 2139 - 2156.
- [4] Ritter, B. and J.-F. Geleyn, 1992: "A comprehensive radiation scheme for numerical weather prediction models with potential applications in climate simulations," *Mon. Wea. Rev.*, 120, 303 - 324.
- [5] Stephens, G. L., P. W. Stackhouse, Jr., and F. J. Flatau, 1990: "The relevance of the microphysical and radiative properties of cirrus clouds to climate and climate feedback," *J. Atmos. Sci.*, 47, 1742 - 1753.
- [6] Mitchell, D. L., A. Macke, and Y. Liu, 1996: "Modeling cirrus clouds. Part II: Treatment of radiative properties," *J. Atmos. Sci.*, 53, 2967 - 2988.
- [7] Clough, S. A., F. X. Kneizys, and R. W. Davies, 1989: "Line shape and the water vapor continuum," *Atmos. Res.*, 23, 229 - 241.
- [8] Lacis, A. A., and V. Oinas, 1991: "A description of the correlated k distribution method for modeling nongray gaseous absorption, thermal emission, and multiple scattering in vertically inhomogeneous atmospheres," *J. Geophys. Res.*, 96, 9027 - 9063.
- [9] Mace, G., R. Marchand, and Q. Zhang, 2004: Level 2B GEOPROF Process Description and Interface Control Document, NASA Jet Propulsion Laboratory, Pasadena, CA, 43 pp.